All-sky limits on Sterile Neutrino Galactic Dark Matter

E. I. Zakharov, **V. V. Barinov**, R. A. Burenin, D. S. Gorbunov, R. A. Krivonos, et al.

Yerevan, Armenia

7 October 2023

Motivation

- The recently launched Spectrum-Roentgen-Gamma space observatory (SRG), carrying two X-ray telescopes on board, ART-XC and eROSITA, is expected to contribute considerably to cosmology by investigating cosmic large scale structure properties associated with galaxy clusters, providing a major improvement in cosmological constraints as compared to the results from earlier X-ray, Sunyaev-Zeldovich and optical galaxy cluster surveys
- These studies can further refine the parameters of Standard Cosmological Model (ΛCDM), the SRG has also high potential in testing specific particle physics models of dark energy and dark matter

Universe Content

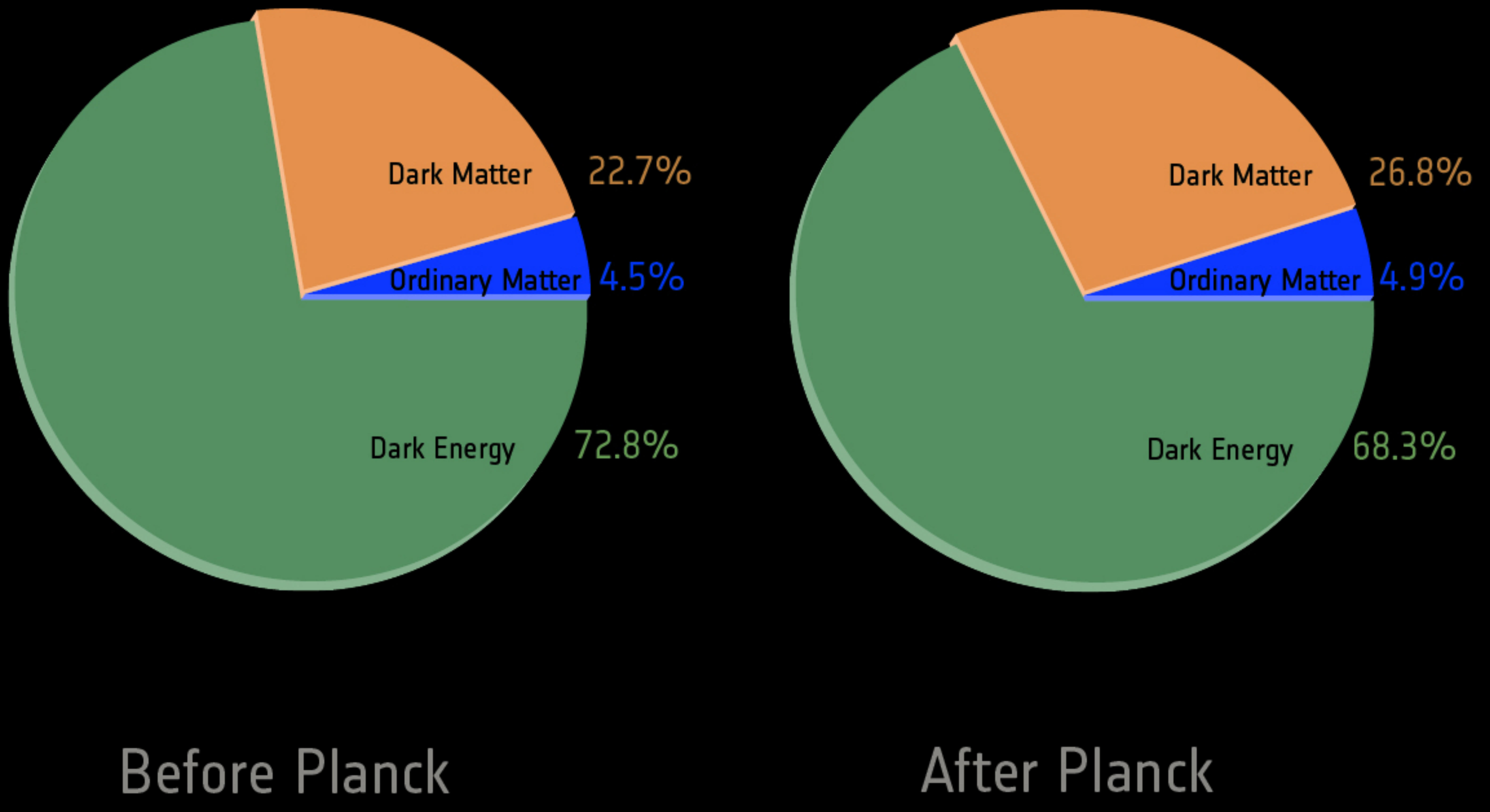

credit: https://sci.esa.int/web/planck/-/51557-planck-new-cosmic-recipe

Dark Matter Candidates

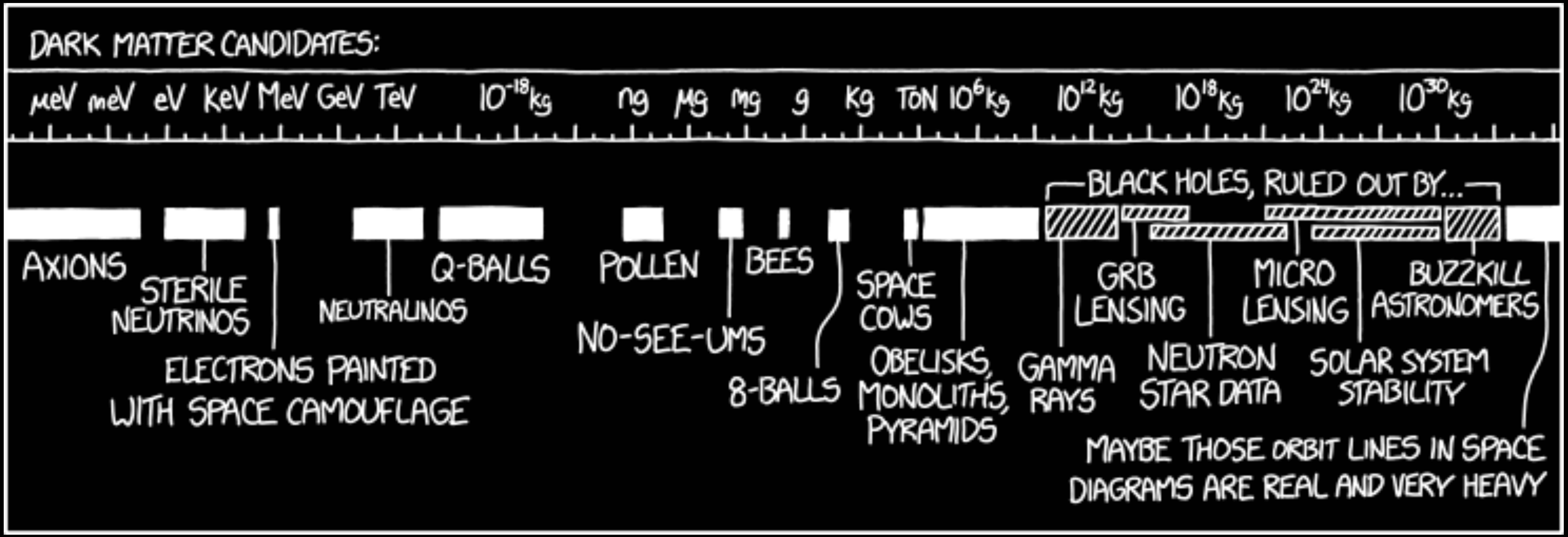

https://www.explainxkcd.com/wiki/index.php/File:dark_matter_candidates.png

Dark Matter Candidates: Sterile Neutrinos

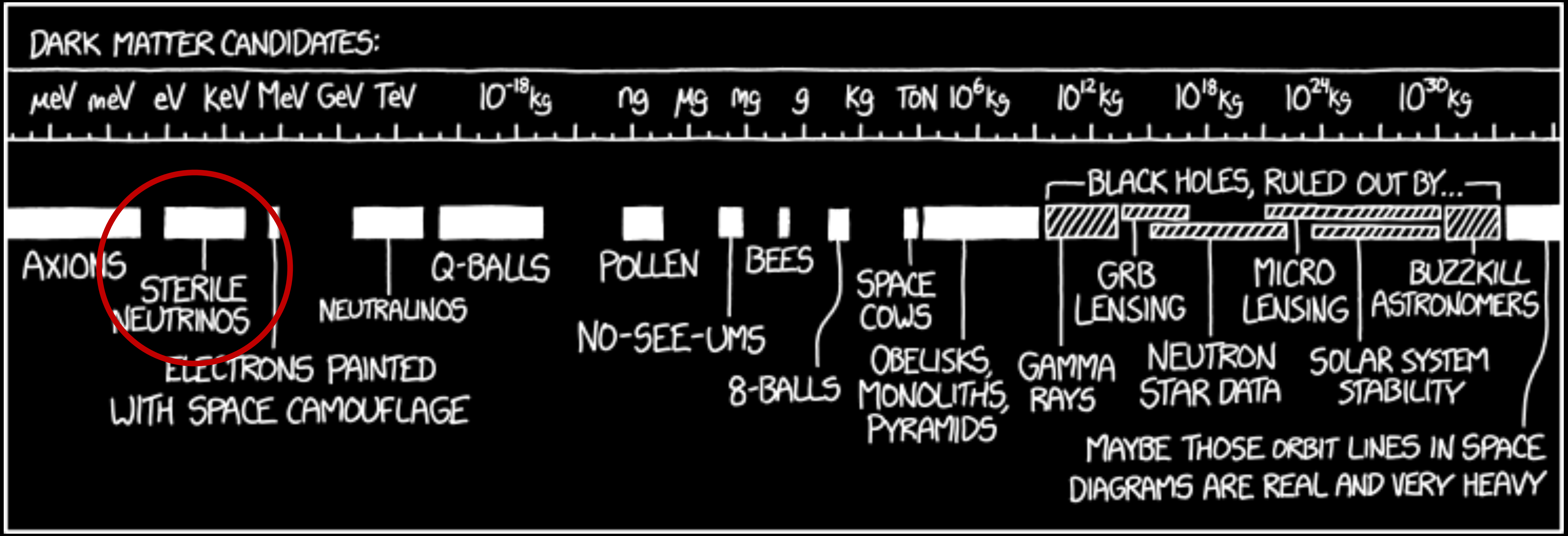

https://www.explainxkcd.com/wiki/index.php/File:dark_matter_candidates.png

Decaying Sterile Neutrinos

We concentrate on a particular candidate of dark matter—sterile neutrinos—unstable because of mixing with active neutrinos and consequently exhibiting a two-body radiative decay into active neutrino and photon

$$\nu_s = \nu_{e,\mu,\tau} + \gamma$$

Decay Rate:

$$\Gamma = \frac{9}{1024}\frac{\alpha}{\pi^4}G_F^2 m_s^5 \sin^2(2\theta) = 1.36 \times 10^{-22}\left(\frac{m_s}{1\ keV}\right)^5 \sin^2(2\theta)\ [s^{-1}]$$

The outgoing photon energy is

$$\mathrm{E}_\gamma = \mathrm{m_s}/2$$

Search Strategy

- Local Astrophysical Observations

  —> Milky Way Observations, Galaxies, Galaxy Clusters

- Cross-Correlation Analysis

  —> Angular power spectra, Line Intensity Mapping

Search Strategy

- ★ Local Astrophysical Observations

  —> Milky Way Observations, Galaxies, Galaxy Clusters

- ★ Cross-Correlation Analysis

  —> Angular power spectra, Line Intensity Mapping

Search Strategy / Local Astrophysical Observations

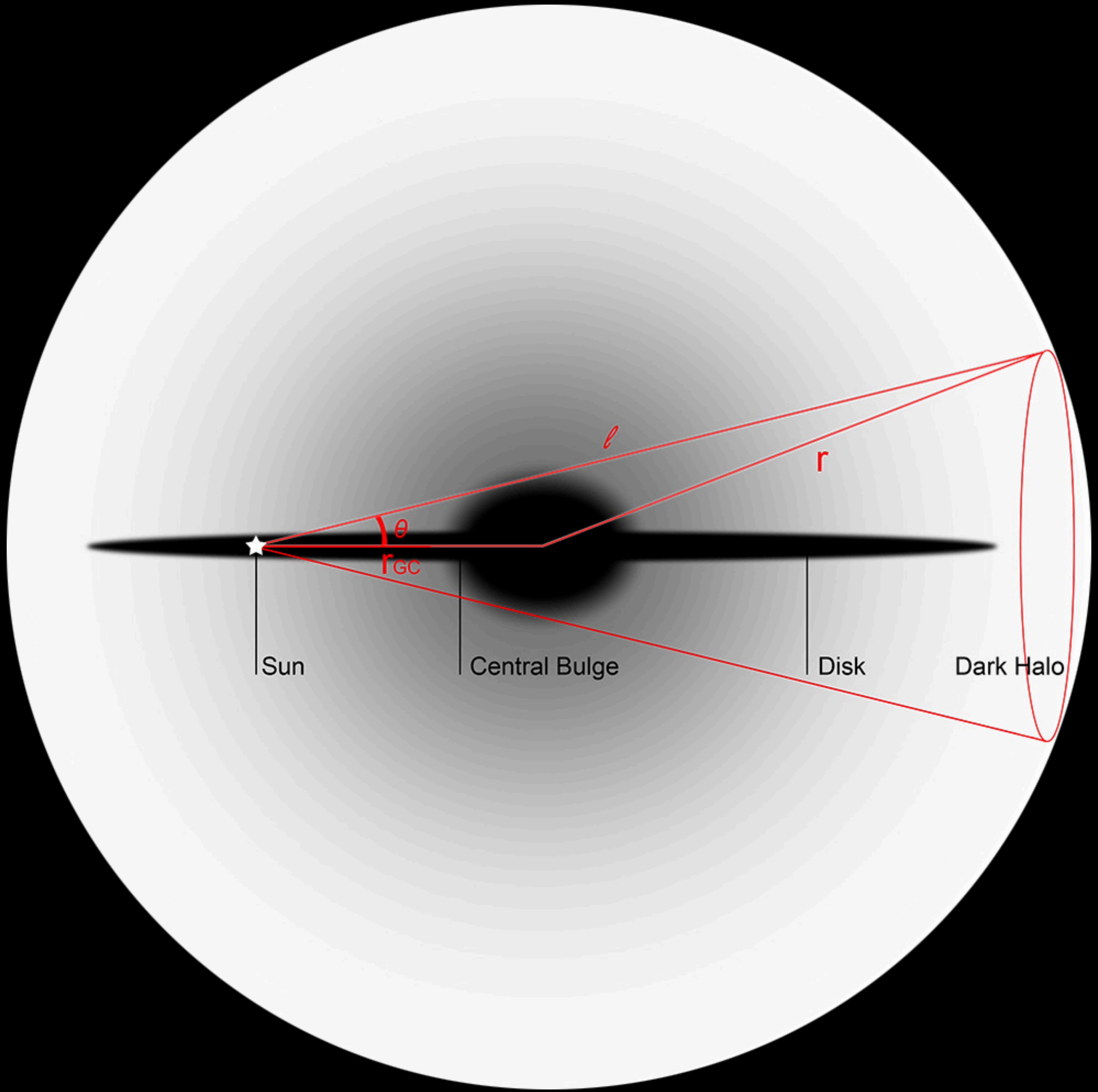

$$F_{DM} = \frac{1}{4\pi}\frac{\Gamma}{m_s}S_{DM}$$

$$S_{DM} = \int_0^{2\pi}\int_0^{\omega_r}\int_0^{\infty}\frac{\rho_{DM}(r(l,\theta))}{l^2}l^2\sin(\theta)d\theta d\phi dl$$

$$r(l,\psi) = \sqrt{R^2 + l^2 - 2Rl\cos(\theta)}$$

$$F_{DM} = \frac{1}{7.88\times10^{-4}}\left(\frac{S_{DM}}{M_{sun}pc^{-2}}\right)\left(\frac{2E_\gamma}{1\ keV}\right)^4\sin^2(2\theta)$$

Dark Matter Density Distribution

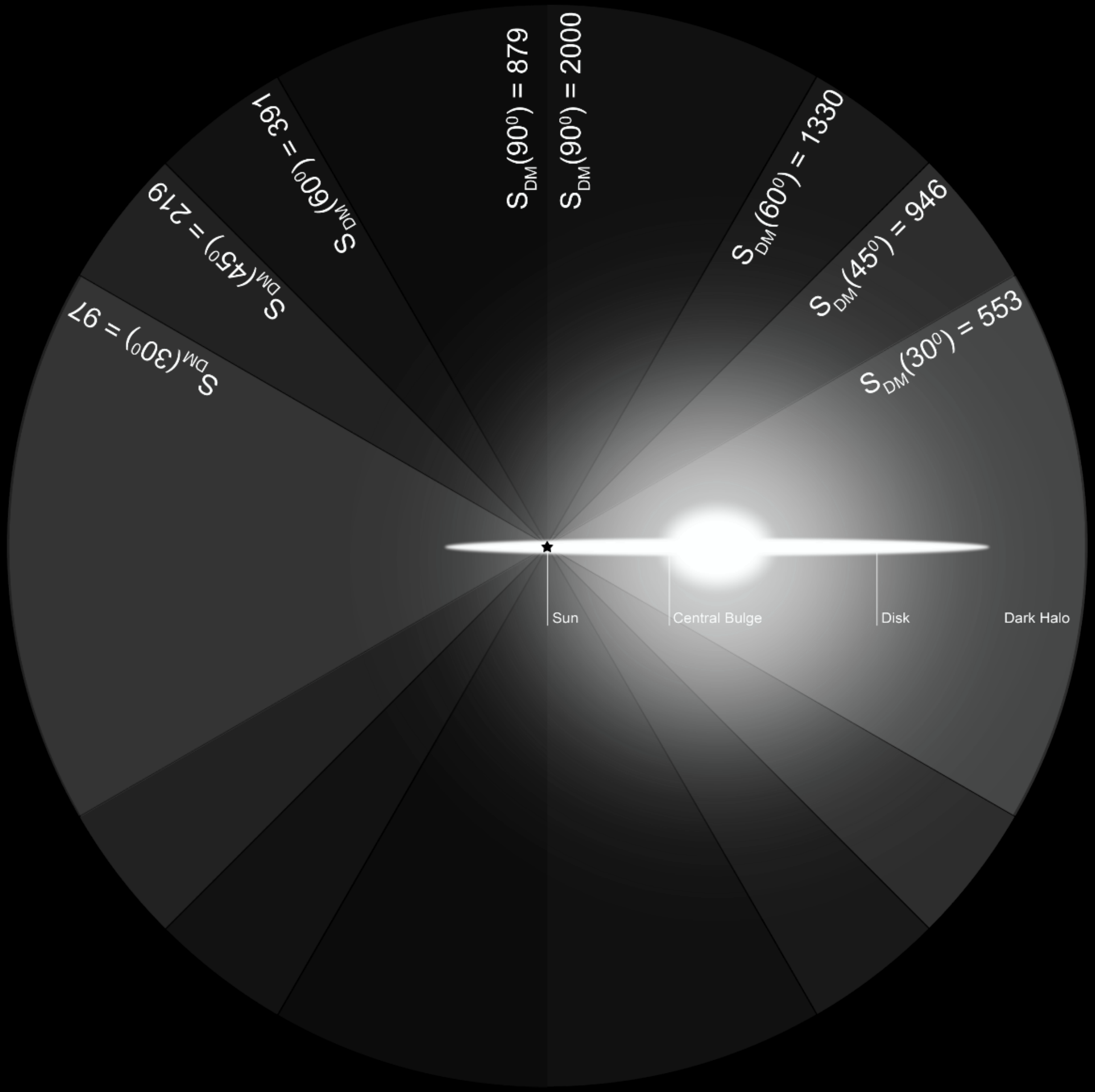

Dark Matter Density Map

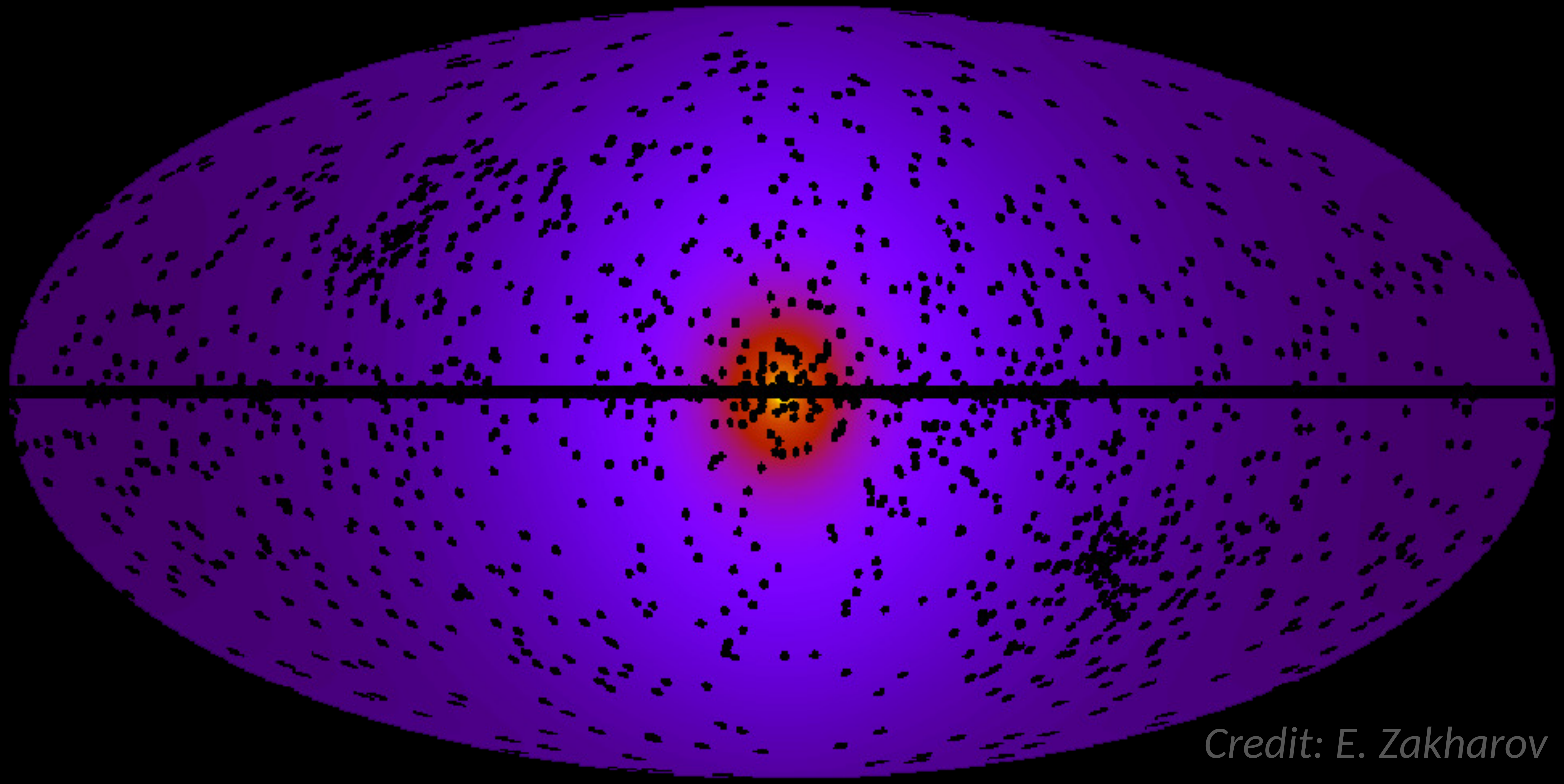

Credit: E. Zakharov

$$S_{DM} = 2\pi \int_0^{\omega_r} \int_0^{\infty} \rho_{DM}(r(l,\theta))\sin(\theta)d\psi dl,$$

NFW profile: $\rho_{DM}(r) = \dfrac{\rho_s}{\left(\frac{r}{r_s}\right)\left(1+\frac{r}{r_s}\right)^2}$

SRG Technical performance

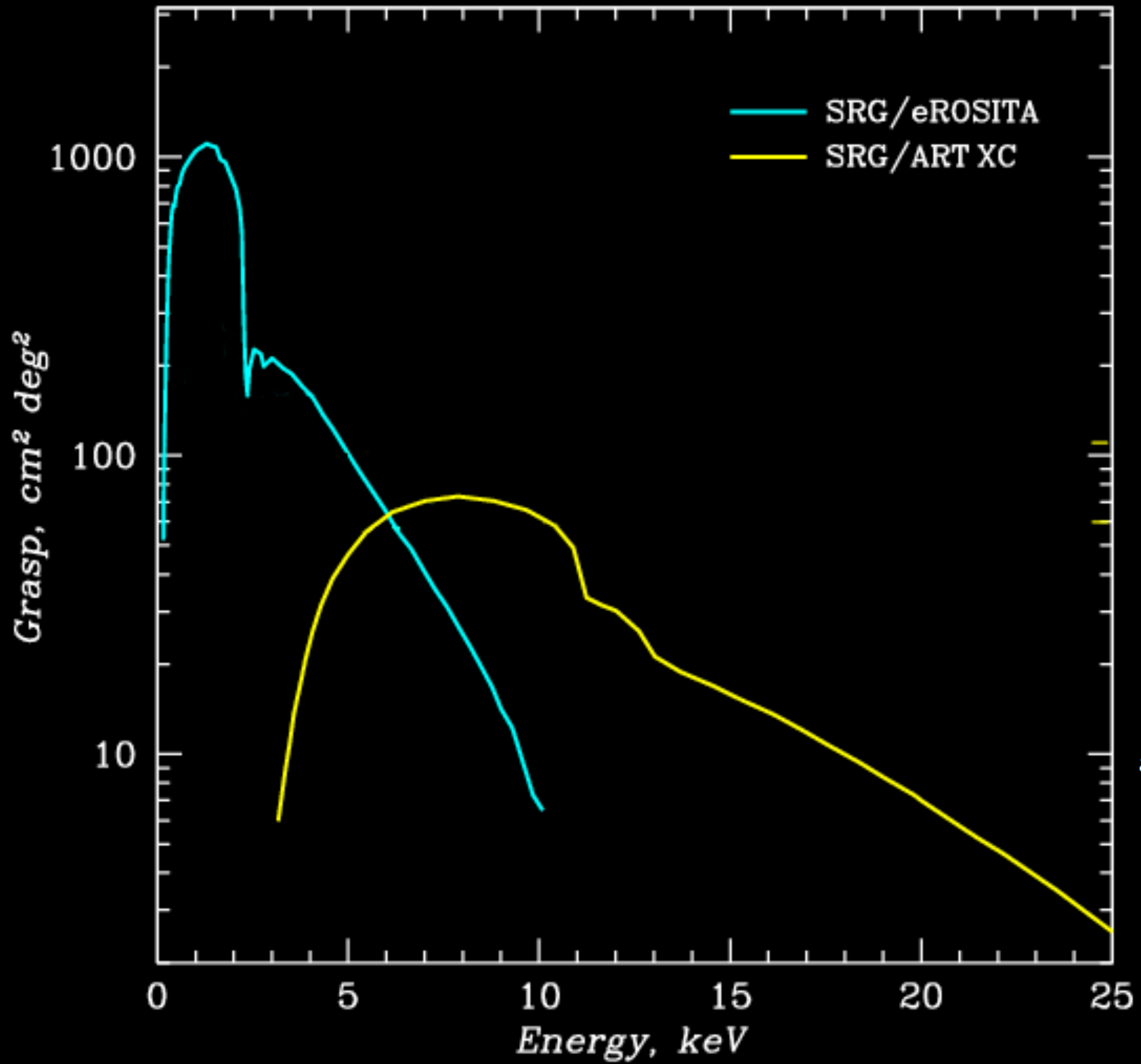

TABLE I. Telescopes technical performance.

	eROSITA	*ART-XC*
energy range [keV]	0.2 – 10	4 – 30
energy resolution, FWHM	138 eV at 6 keV	10% at 14 keV
field of view (FOV) [deg^2]	0.833	0.3 – 2.0 [a]

[a] FOV [deg^2]: Telescope 0.31, Concentrator 1.7, Full 2.0 [3–5].

Expected SRG Constraints for 4yr Observations around MW Center

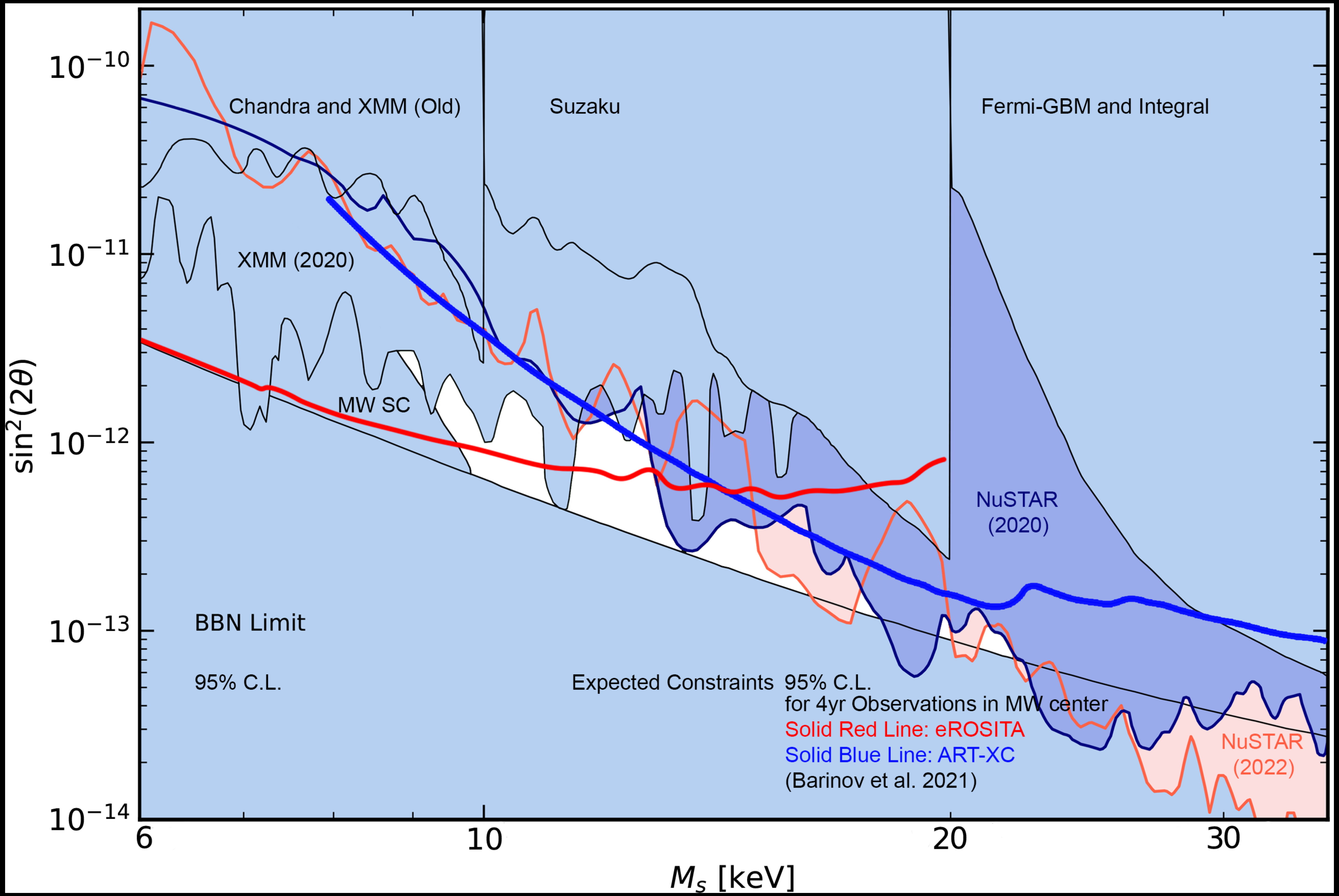

SNR

95% Expected Upper Limits

for Given Time

$$\frac{F_{DM}\left(\frac{G(E)}{\Omega}\right)T_{obs}}{\sqrt{F_{DM}\left(\frac{G(E)}{\Omega}\right)T_{obs}+C_{BG}T_{obs}}} = \sigma,\ d.o.f. = 1$$

What about actual observational data?

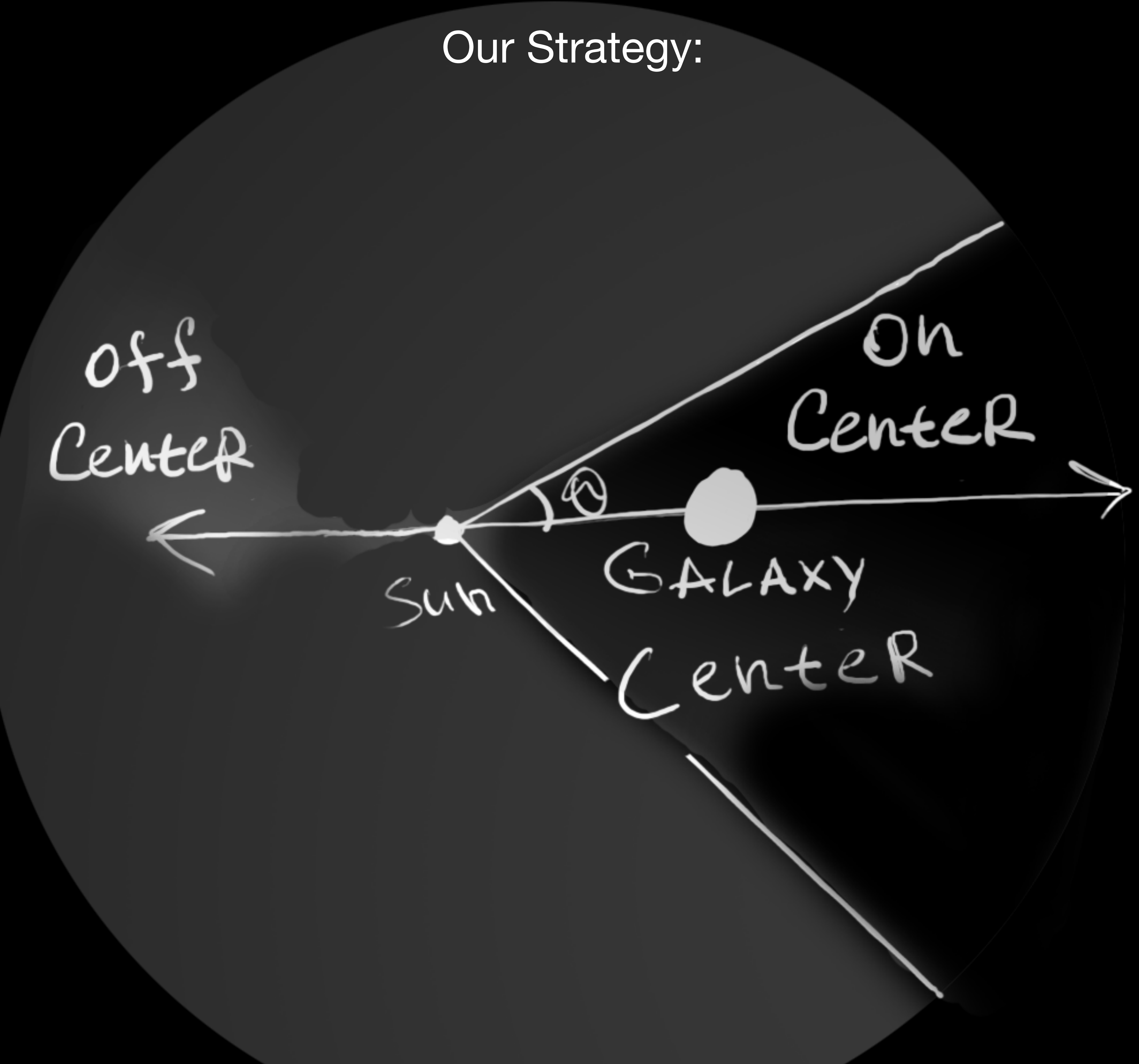

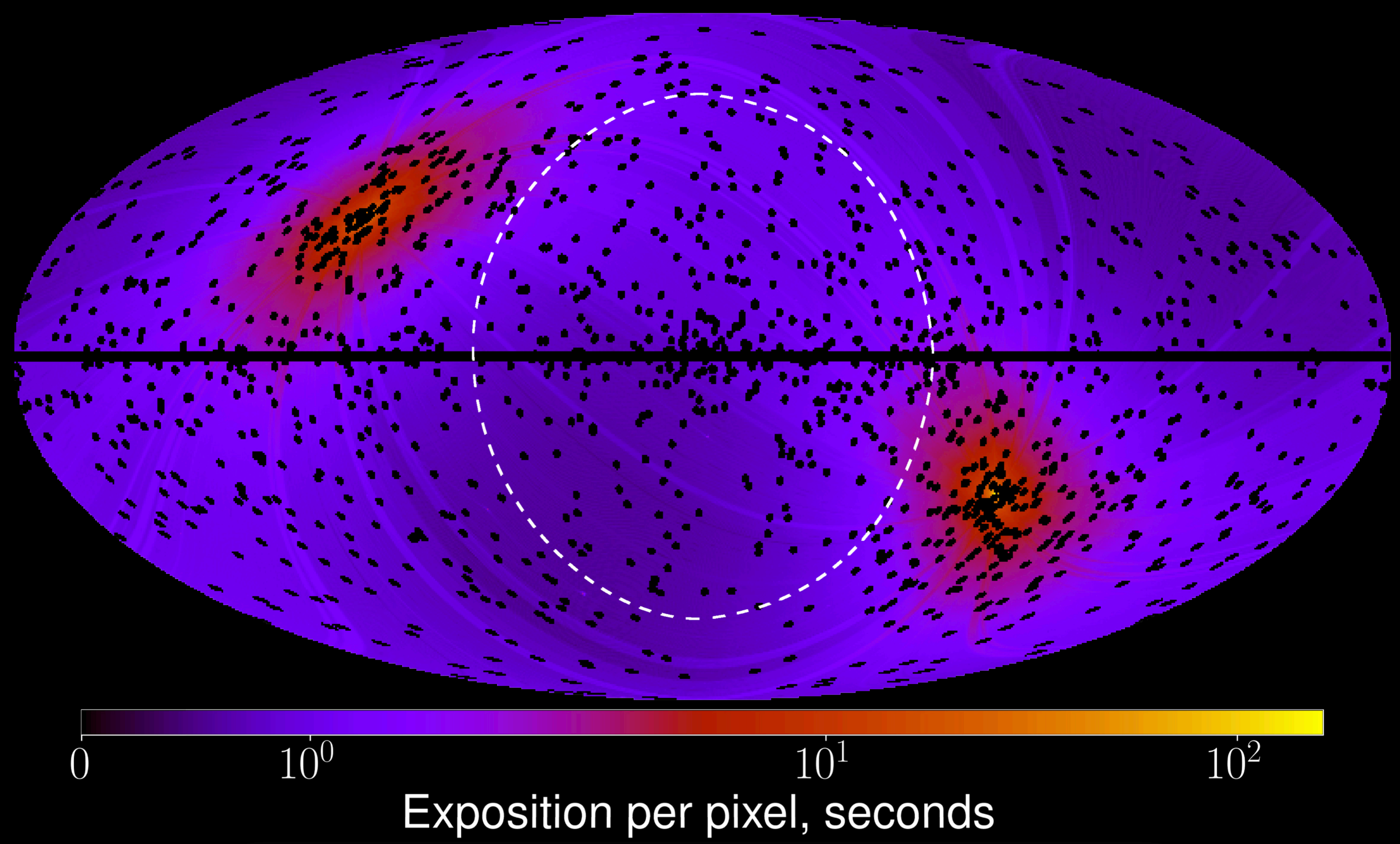

FIG. 2. The two-year all-sky exposure $\epsilon(\phi, \psi)$ of *ART-XC* used in this analysis. The regions excluded from our analysis are shown in black. White dashed circle denotes the border between the region I (inner area, $\Omega^I \approx 9040\,\mathrm{deg}^2$) and region II (outer area, $\Omega^{II} \approx 27600\,\mathrm{deg}^2$). Regions I and II comprise exposure time of $T^I \approx 10.6\,\mathrm{Ms}$ and $T^{II} \approx 42.5\,\mathrm{Ms}$, respectively.

Background + Possible Signal Subtraction

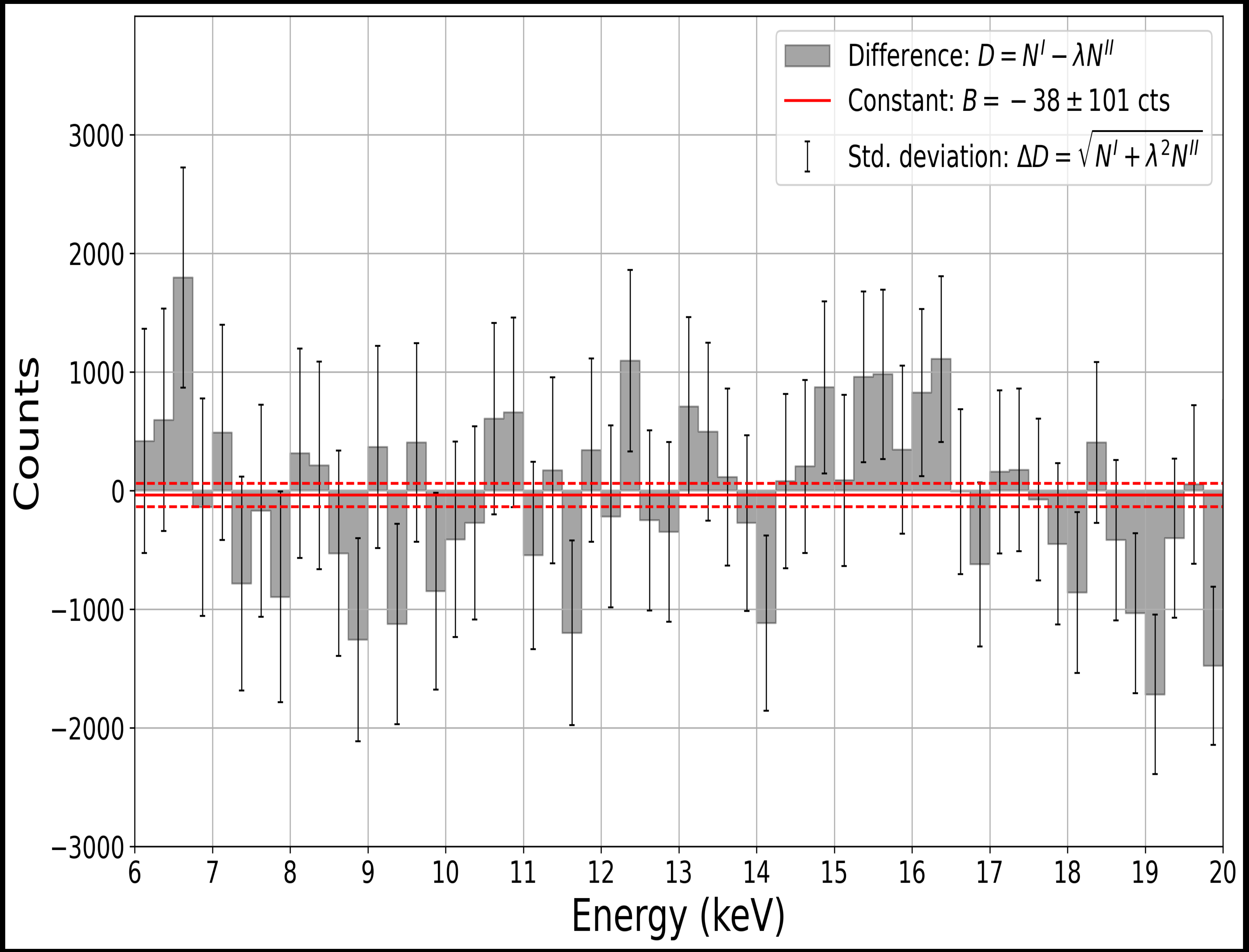

$$D_i \equiv N_i^I - \lambda N_i^{II}$$

$$l(D|A,E) = \sum_{i=1}^{N^b} \frac{(D_i - B - S_i(A,E))^2}{2\sigma_i^2},$$

$$S_i = \frac{A \times 2\sqrt{\log 2}}{\sqrt{\pi}\mathrm{FWHM}(E)} \exp\left(-\left(\frac{2(E_i - E)}{\mathrm{FWHM}(E)}\right)^2 \log 2\right)\Delta E$$

$$\frac{A\Omega^I}{T^I G(E)} = F^I - \lambda F^{II}$$

All-sky limits on Sterile Neutrino Galactic Dark Matter **obtained** with SRG/ART-XC after two years of operations

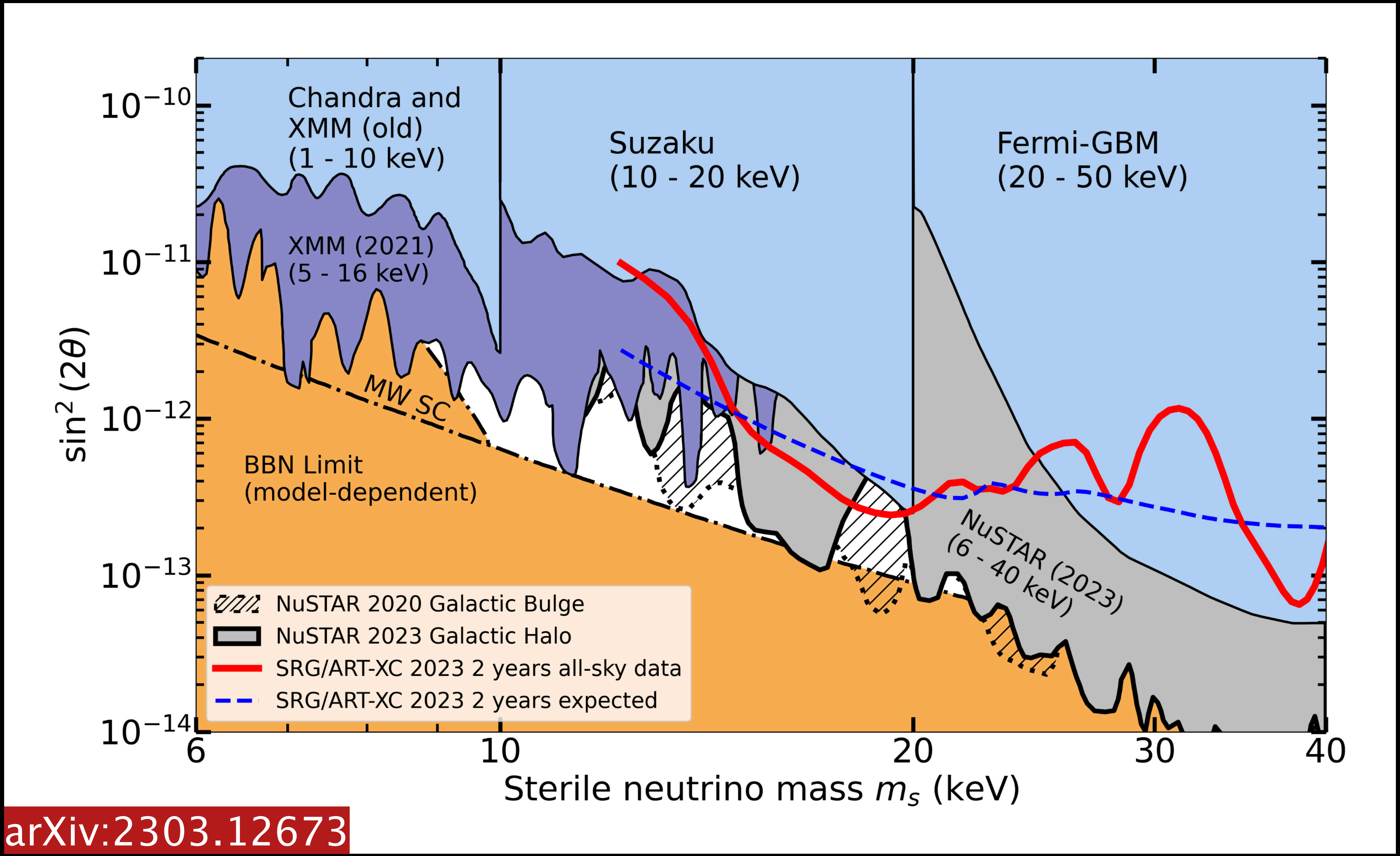

Upper Limits

95% C.L.

$\Delta\chi^2 = 2.71$

Prospects

The further prospects of ART-XC in exploring the sterile neutrino DM are related to the use of ART-XC data obtained during its Galactic Plane survey, undertaken in 2022–2023, with more than a year total exposure. Also we plan to use the next 2-year ART-XC all-sky survey, which is planned to be started in 2023.

The other important SRG dataset, are the data of eROSITA survey, which should allow for exploring sterile neutrino DM in softer, 0.5–8 keV energy range, while in 4-8 keV energy range, covered by the both SRG telescopes, the joint analysis of the data from both ART-XC and eROSITA is possible. The analysis of the fluxes from nearby galaxy clusters (e.g. Coma) and analysis of the contribution of unresolved X-ray sources along the lines can additionally strengthen the constraint on the model parameters of the sterile neutrino DM.

We expect that these data will significantly improve our current ART-XC constraints on the decay of the sterile neutrino DM.

Search Strategy

- ★ **Local Astrophysical Observations**

  —> Milky Way Observations, Galaxies, Galaxy Clusters

- ★ **Cross-Correlation Analysis**

  —> Angular power spectra, Line Intensity Mapping

Search Strategy / Cross-correlation analysis

- Because dark matter particles are concentrated within galaxies and galaxy clusters, each photon from a dark matter detection should lead to a specific object (structure) where decay occurs.

- If the photons were not deflected, then they point to part of this structure in the sky. Including the spatial distribution of this structure due to redshift.

- Even if the object cannot be detected by the observer so far (unresolved sources), the connection between the photon and its effect exists and can be traced statistically, through a joint analysis of the distribution of all registered photons according to the dynamics of arrival, energy and map structure.

Cross-Correlation Analysis

- This approach is based on studying the auto- and cross-correlation angular power spectrum of dark matter and galaxies.

- As part of the correlation analysis, for each pair of signatures (dark matter - dark matter, galaxies - galaxies, dark matter - galaxies), a nonlinear power spectrum is calculated, and then a cross-correlation function is constructed for all pairs of signatures under study.

$$\langle \delta I_i(\vec{n_1}) \delta I_j(\vec{n_2}) \rangle = \sum_l \frac{2l+1}{4\pi} \boxed{C_l^{ij}} P_l(cos(\theta))$$

$$\delta I_i(\vec{n}) = I_i(\vec{n}) - \langle I_i \rangle$$

Averaged Intensity over the sky

$$I_{\rm dm}(E) = \int_0^\infty {\rm d}\chi W_{dm}(E, z)$$

Cross - Correlation Analysis

The angular correlation power spectrum is the Fourier image of the two-point correlation function for given signatures. It determines the magnitude and properties of the anisotropy of the signatures (signature) and is given by the following expression:

$$C_l^{ij} = \frac{2}{\pi} \int_0^\infty \mathrm{d}\chi \int_0^\infty \mathrm{d}\chi' \int_0^\infty k^2 \mathrm{d}k \, \overline{W}_i(\chi) \, \overline{W}_j(\chi') \, P_{ij}\left(k, \chi, \chi'\right) \, j_l(k\chi) j_l(k\chi')$$

In the Limber Approximation (l >> 1)

$$C_l^{ij} = \int_0^\infty \frac{\mathrm{d}\chi}{\chi^2(z)} \overline{W}_i(\chi) \overline{W}_j(\chi) \, P_{ij}\left(k \approx \frac{l}{\chi}, z\right), \, l \gg 1, \, l \approx kr = k\chi$$

$$\overline{W}_i(z) = \int_{E_{min}}^{E_{max}} \mathrm{d}E W_i(E, z)$$

$$W_g(z) = \frac{\mathrm{d}z}{\mathrm{d}\chi} \left[\frac{1}{N_{2\mathrm{MRS}}} \frac{\mathrm{d}N_{2\mathrm{MRS}}}{\mathrm{d}z} \right]$$

$$W_{\mathrm{dm}}(E, z) = \frac{\Omega_{\mathrm{CDM}} \rho_{crit}}{(1+z)} \frac{\Gamma_{\nu_s}}{4\pi m_{\nu_s}} \frac{1}{\sqrt{2\pi\sigma_E^2}} \exp\left[-\frac{\left(E - \frac{m_{\nu_s}}{2(1+z)}\right)^2}{2\sigma_E^2} \right]$$

$$P_{ij}\left(k, \chi, \chi'\right) = \sqrt{P_{ij}\left(k, \chi\right) P_{ij}\left(k, \chi'\right)}$$

Halo Model

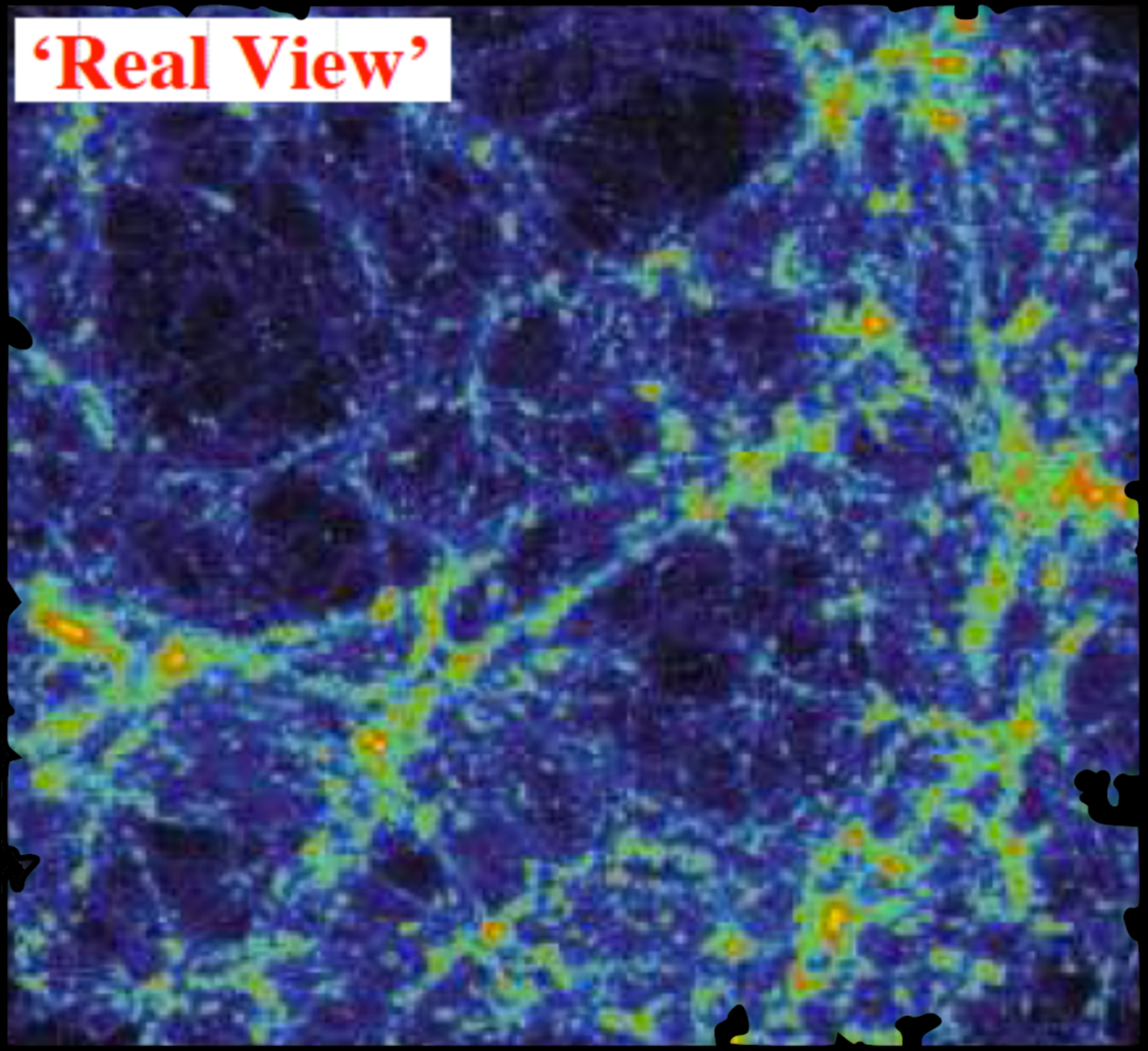

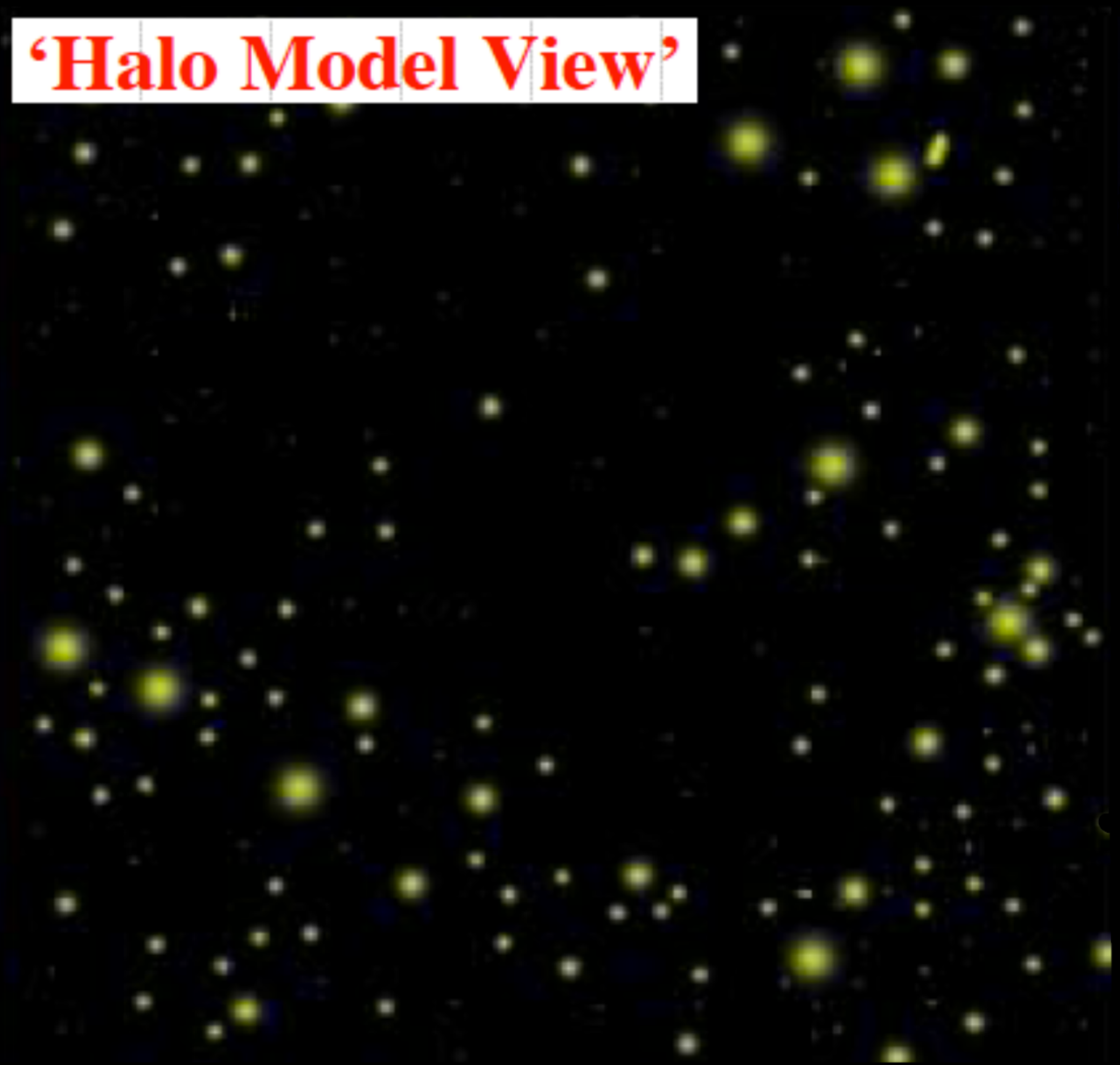

credit: ASTR 610: Theory of Galaxy Formation © Frank van den Bosch, Yale University

Halo Model

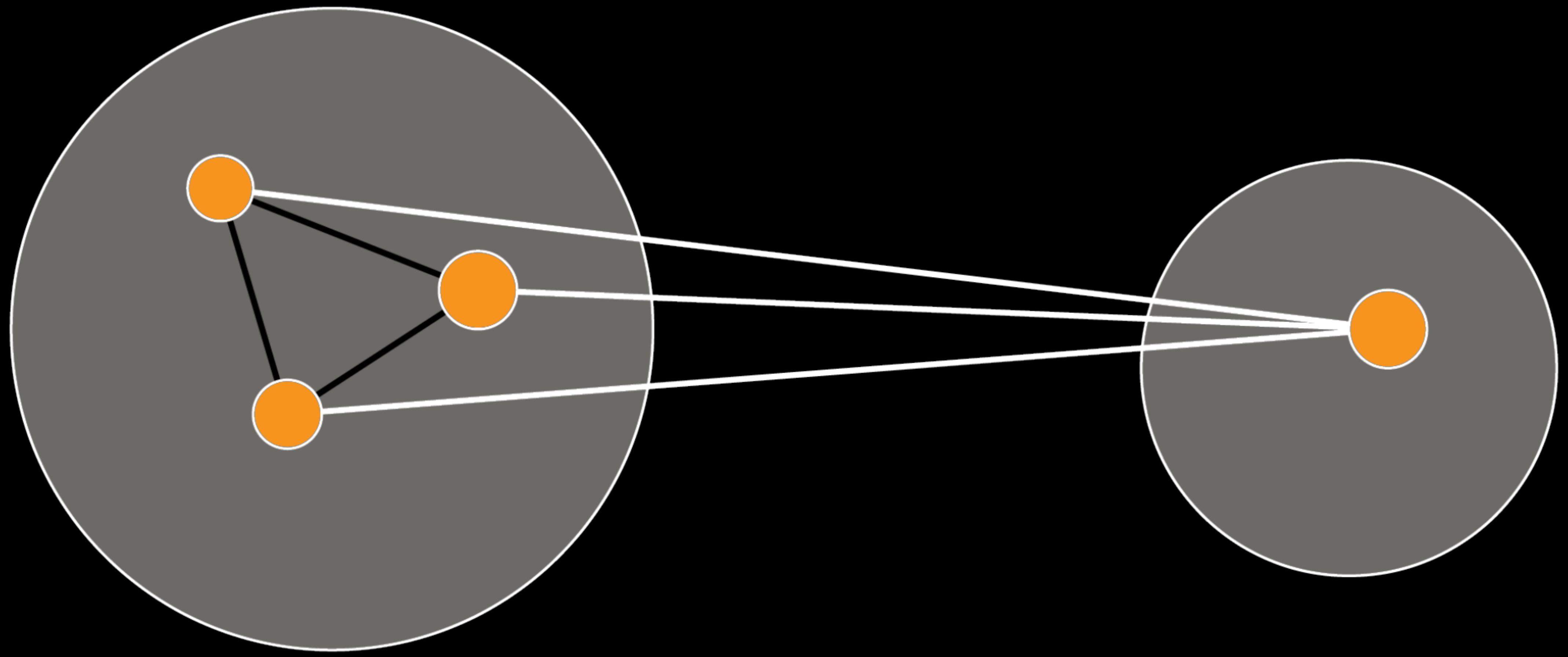

$$C_l^{dm,g} = \int_0^\infty \frac{\mathrm{d}\chi}{\chi^2} \overline{W}_{dm}(\chi) W_g(\chi) \; P_{dm,g}\left(k = \frac{l}{\chi}, z\right)$$

$$P_{ij}(k,z) = P_{ij}^{1h}(k,z) + P_{ij}^{2h}(k,z)$$

$$P_{\mathrm{dm,\ g}}(k,z) = P_{\mathrm{dm,\ g}}^{1h}(k,z) + P_{\mathrm{dm,\ g}}^{2h}(k,z)$$

$$P_{ij}^{1h}(k,z) = \int \mathrm{d}M \frac{\mathrm{d}n(M,z)}{\mathrm{d}M} \left(\frac{M}{\bar{\rho}(z)}\right)^2 u_i^*(k;M,z) u_j(k;M,z),$$

$$P_{ij}^{2h}(k,z) = \left[\int \mathrm{d}M_1 \frac{\mathrm{d}n(M_1,z)}{\mathrm{d}M_1} \left(\frac{M_1}{\bar{\rho}(z)}\right) b_i(M_1,z) u_i^*(k;M_1,z)\right] \times \left[\int \mathrm{d}M_2 \frac{\mathrm{d}n(M_2,z)}{\mathrm{d}M_2} \left(\frac{M_2}{\bar{\rho}(z)}\right) b_j(M_2,z) u_j(k;M_2,z)\right] P_{\mathrm{lin}}(k,z)$$

$$P_{\mathrm{dm,\ g}}^{1h}(k,z) = \int \mathrm{d}M \frac{\mathrm{d}n(M,z)}{\mathrm{d}M} \frac{\langle N_g \rangle_M}{\langle n_g(z) \rangle} u_{\mathrm{g}}(k;M,z) \left(\frac{M}{\bar{\rho}(0)}\right) u_{\mathrm{dm}}(k;M,z)$$

$$P_{\mathrm{dm,\ g}}^{2h}(k,z) = \left[\int \mathrm{d}M \frac{\mathrm{d}n(M,z)}{\mathrm{d}M} b_{\mathrm{lin}}(M;z) \left(\frac{M}{\bar{\rho}(0)}\right) u_{\mathrm{dm}}(k;M,z)\right] \times \left[\int \mathrm{d}M \frac{\mathrm{d}n(M,z)}{\mathrm{d}M} b_{\mathrm{lin}}(M;z) \frac{\langle N_g \rangle_M}{\langle n_g(z) \rangle} u_{\mathrm{g}}(k;M,z)\right] P_{\mathrm{lin}}(k,z)$$

Data Analysis

$$\chi^2 = \sum_{l,l',E,E'} \left(C^{\rm dm,g}_{l,E} - C^{\rm m}_{l,E} \right) \left(\delta C^2_{l,l',E,E'} \right)^{-1} \left(C^{\rm dm,g}_{l',E'} - C^{\rm m}_{l',E'} \right)$$

We set X2=2.71 for the 95% C.L. Upper Limits

$$\delta C^2_{l,l',E,E'} = \frac{\delta_{l,l'}}{(l+1/2) l f_{sky}} \left(C^{\rm dm,g}_{l,E} C^{\rm dm,g}_{l',E'} + \left(C^{\rm dm,dm}_{l,E,E'} + C^{\gamma}_{N,E} \delta_{E,E'} \right) \left(C^{\rm g,g}_{l'} + C^{\rm g}_{N} \right) \right)$$

$$C^{\gamma}_{N,E} = \frac{4\pi f_{sky}}{W_l^2} \frac{\overline{I_\gamma}^2}{N_E}$$

The shot noise due to X-ray photons

$$N_E = T_{obs} \Omega_{\rm FOV} f_{sky} \int_{E_{min}}^{E_{max}} {\rm d}E I_\gamma(E) A_{eff}(E)$$

$$C^g_N = \frac{4\pi f_{sky}}{N_g}$$

Galaxies shot noise term

Example: Cross-correlation angular power spectrum for the eROSITA Telescope

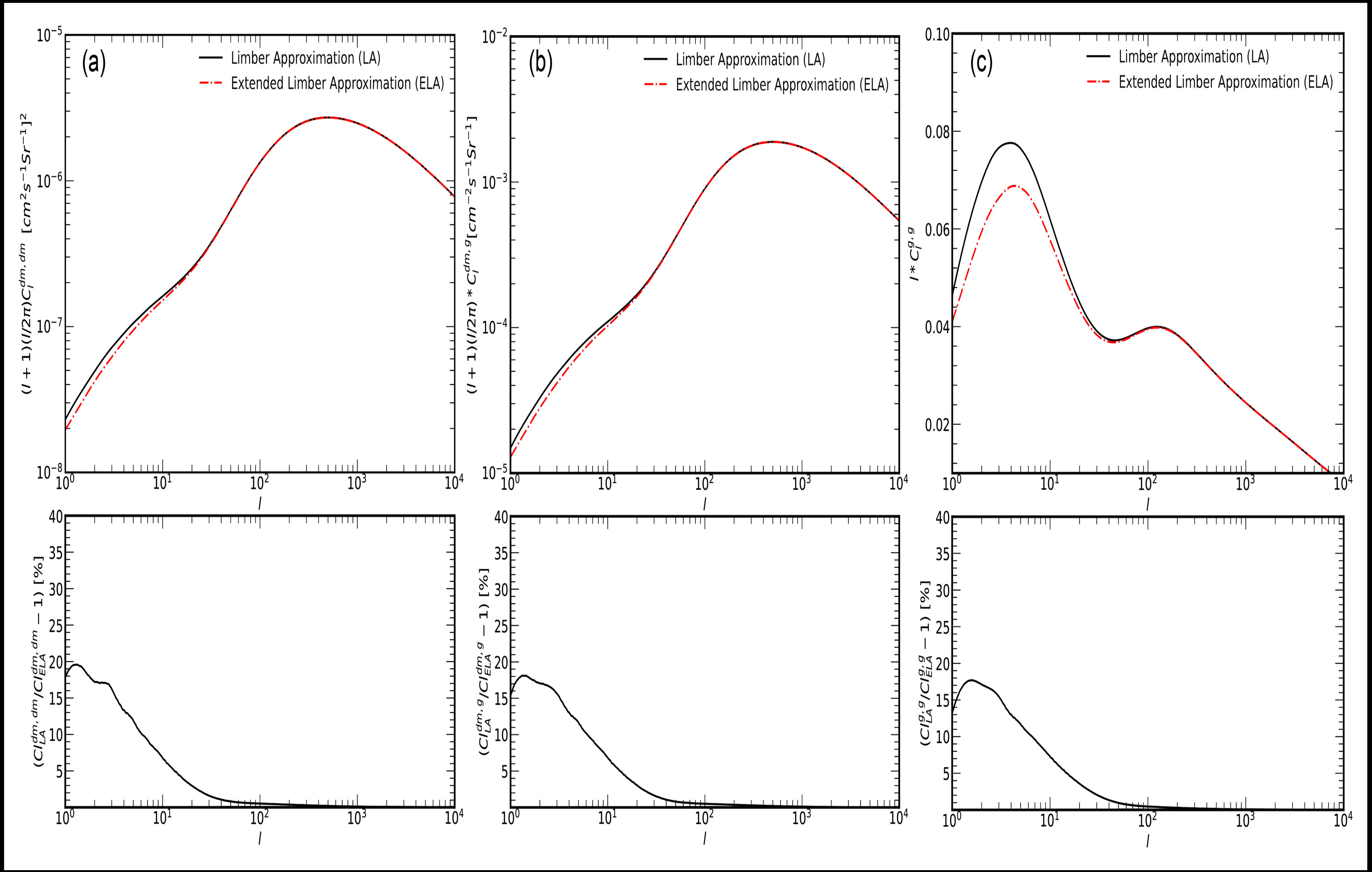

Panel (**a**): Autocorrelation angular power spectrum of dark matter due to dark matter particle decays.

Panel (**b**): Cross-correlation angular power spectrum of dark matter and galaxies, plotted for the 2MRS catalog using the HOD formalism.

Panel (**c**): Autocorrelation angular power spectrum of galaxies constructed for the 2MRS catalog using the HOD formalism.

These spectra are plotted for sterile neutrino parameters (m = 7.12 keV, sin2(2θ)) = 7.6×10-11), where the energy range for the average X-ray photon emission intensity is [3.4, 3.6] keV.

The bottom panels show the difference between the Limber approximation and the extended Limber approximation.

Previous expected constraints for eROSITA telescope

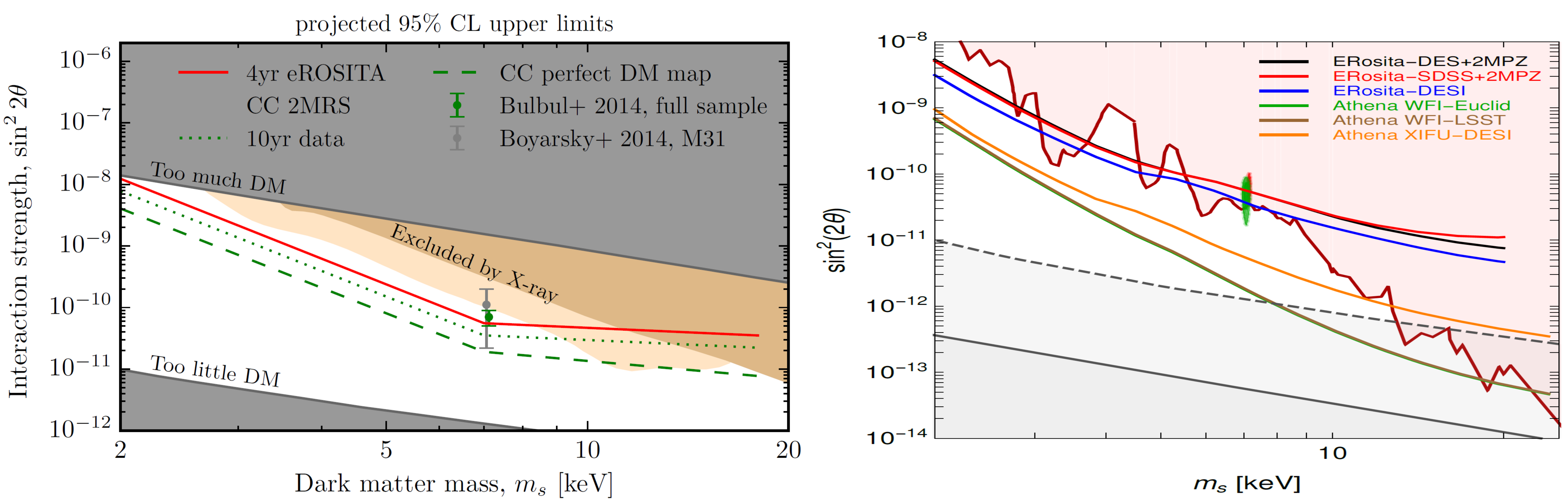

F. Zandanel et al, arXiv:1505.07829v3 Andrea Caputo et al, arXiv:1911.09120v3

Expected constraints on sterile neutrino parameters for eROSITA and ART-XC telescopes from cross-correlation analysis for 4yr observations

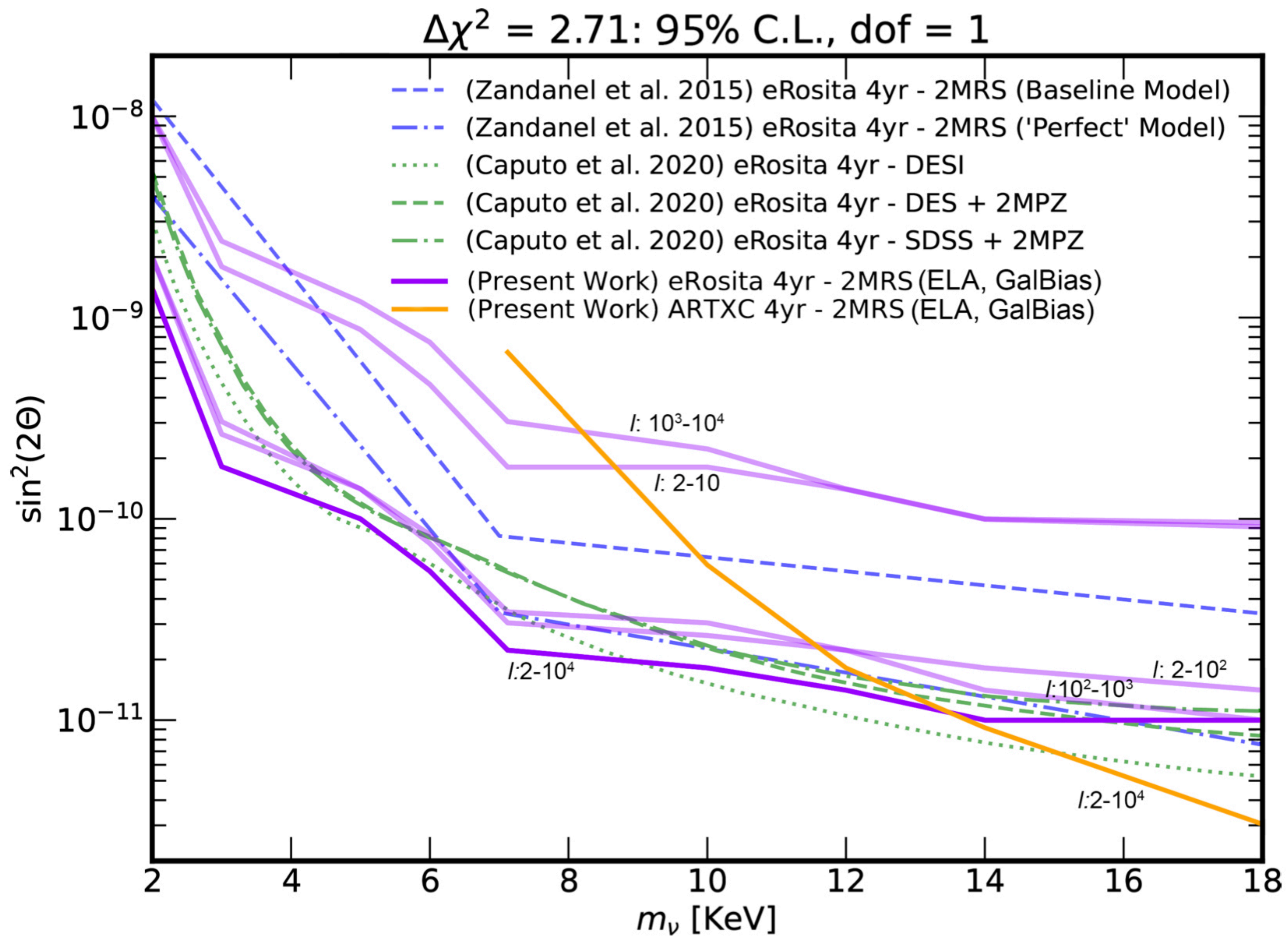

Figure 2. Expected constraints on the parameters of sterile neutrinos obtained in the framework of our analysis for various ranges of multipoles. The purple line corresponds to the constraints for the eROSITA telescope (the translucent purple lines show the contributions to the constraints for different ranges of multipoles). The yellow line corresponds to the ART-XC telescope. For comparison, the constraints from the works [27, 28] are presented. The observation time is 4 years in the full sky survey mode.

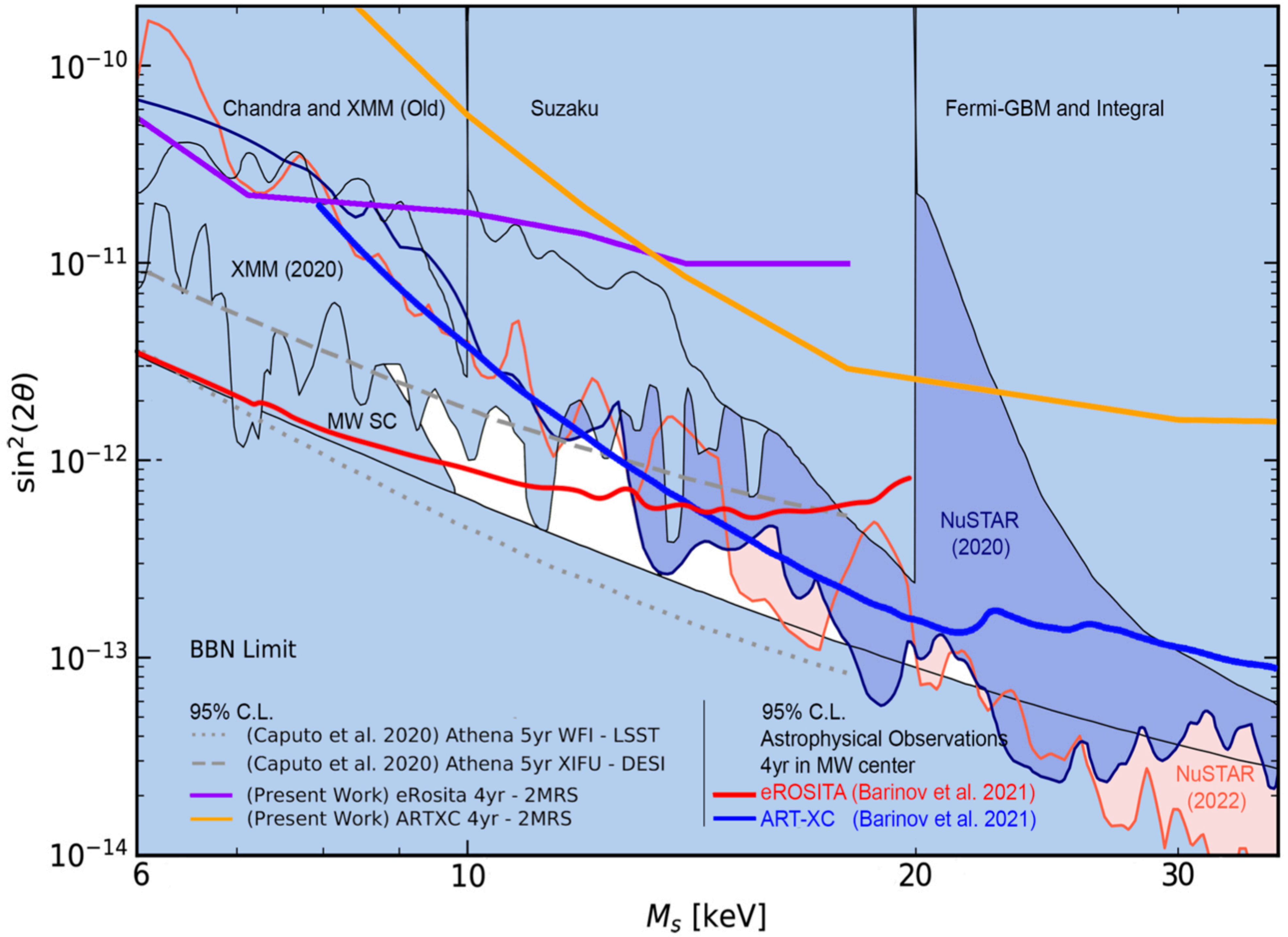

Figure 3. Expected Constraints on the parameters of sterile neutrinos obtained in our analysis (same as Figure 2) in comparison with the constraints that can be obtained in the framework of the astrophysical observations of the center of the Milky Way in a cone with an opening angle of 60 degrees [45] (the red line corresponds to the constraints for the eROSITA telescope, the blue line corresponds to the ART-XC telescope). Background Corrected means that the background has been additionally normalized taking into account additional features for the ART-XC telescope [43] compared to the previous work [45]. Additionally, we present the constraints that can be obtained for the Athena telescope [28].

arXiv:2211.05919

Thank you for Your Attention!

This work was supported by RSF 22-12-00271